Swinburne Research Bank
http://researchbank.swinburne.edu.au

Forbes, D. A., Spitler, L. R., & Graham, A. W., et al. (2011). Bridging the gap between low- and high-mass dwarf galaxies.

Originally published in *Monthly Notices of the Royal Astronomical Society*, *413*(4), 2665–2678.
Available from: http://dx.doi.org/10.1111/j.1365-2966.2011.18335.x.

This version of the article copyright © 2011 The Authors.

This is the author's version of the work. It is posted here with the permission of the publisher for your personal use. No further distribution is permitted. If your library has a subscription to this journal, you may also be able to access the published version via the library catalogue.

The definitive version is available at www.interscience.wiley.com.

Accessed from Swinburne Research Bank: http://hdl.handle.net/1959.3/190965

Mon. Not. R. Astron. Soc. **000**, 1–?? (2002) Printed 14 January 2011 (MN LaTeX style file v2.2)

Bridging the gap between low and high mass dwarf galaxies

Duncan A. Forbes[1⋆], Lee R. Spitler[1], Alister W. Graham[1], Caroline Foster[1], G. K. T. Hau[1], Andrew Benson[2]
[1] *Centre for Astrophysics & Supercomputing, Swinburne University, Hawthorn VIC 3122, Australia*
[2] *Mail Code 350-17, California Institute of Technology, Pasadena, CA 91125, USA*

arXiv:1101.2460v1 [astro-ph.CO] 12 Jan 2011

14 January 2011

ABSTRACT

While the dark matter content within the most massive giant and smallest dwarf galaxies has been probed – spanning a range of over one million in mass – an important observational gap remains for galaxies of intermediate mass. This gap covers K band magnitudes of approximately –16 > M_K > –18 mag (for which dwarf galaxies have B–K ∼ 2). On the high mass side of the gap are dwarf elliptical (dE) galaxies, that are dominated by stars in their inner regions. While the low mass side includes dwarf spheroidal (dSph) galaxies that are dark matter-dominated and ultra compact dwarf (UCD) objects that are star-dominated. Evolutionary pathways across the gap have been suggested but remain largely untested because the 'gap' galaxies are faint, making dynamical measurements very challenging.

With long exposures on the Keck telescope using the ESI instrument we have succeeded in bridging this gap by measuring the dynamical mass for five dwarf galaxies with $M_K \sim -17.5$ ($M_B \sim -15.5$). With the exception of our brightest dwarf galaxy, they possess relatively flat velocity dispersion profiles of around 20 km s^{-1}. By examining their 2D scaling relations and 3D fundamental manifold, we found that the sizes and velocity dispersions of these gap galaxies reveal continuous trends from dE to dSph galaxies. We conclude that low-luminosity dwarf elliptical galaxies are dominated by stars, not by dark matter, within their half light radii. This finding can be understood if internal feedback processes are operating most efficiently in gap galaxies, gravitationally heating the centrally-located dark matter to larger radii. Whereas external environmental processes, which can strip away stars, have a greater influence on dSph galaxies resulting in their higher dark matter fractions. UCDs appear to be more similar to massive compact star clusters than to small galaxies. Our dynamical study of low mass dwarf elliptical galaxies provides further constraints on the processes that shape some of the smallest and most numerous galaxies in the Universe.

Key words: galaxies: dwarf – galaxies:star clusters – galaxies:evolution – galaxies: kinematics and dynamics

1 INTRODUCTION

Galaxies are predicted to form within massive halos of dark matter, with the galaxy stellar mass making up only a small fraction of the total mass (e.g. Benson & Bower 2010). In order to measure the total mass of an individual galaxy, and hence probe the actual fraction of dark and stellar matter, one requires a dynamical study. Such studies typically measure the motion of stars well within a projected radius containing half of the total galaxy light (called the half light or effective radius R_e). For galaxies that are dominated by random motions in their inner regions, past dynamical studies have ranged from the most massive elliptical galaxies to the lowest mass dwarfs. However, a single gap exists for which no dynamical studies are currently available.

This mass gap represents a key transition region from high mass dwarf elliptical (dE) galaxies that are stellar mass dominated in their inner regions (de Rijcke et al. 2006; Toloba et al. 2010) to dwarf spheroidal (dSph) galaxies that are dark matter dominated (e.g. Wolf et al. 2010) and ultra compact dwarf (UCD) objects that are dominated by stars (Dabringhausen et al. 2008; Forbes et al. 2008; Mieske et al. 2008). These systems are all largely devoid of gas, consist of old age stars, have smooth featureless morphologies and are

⋆ E-mail: dforbes@swin.edu.au

pressure-supported by random internal stellar motions. The relationship between these three types of dwarf systems is a subject of active debate.

Here we define the gap, somewhat subjectively, to be dwarf galaxies less massive than the lowest mass dE studied to date (Geha et al. 2003; Chilingarian 2009) and more massive than the Fornax dwarf spheroidal galaxy (the most massive in the Local Group). In terms of absolute K band magnitude this corresponds to roughly $-16 > M_K > -18$ mag. Over this magnitude range dwarf ellipticals have colours of B–K $\sim$ 2 (Forbes et al. 2008). With this definition of the gap, two of the Local Group dE galaxies (i.e. NGC 147 and 185) lie within the gap.

Despite being numerous in the Universe, our Local Group of galaxies contains only three dEs. All three have been classified as peculiar due to their ongoing interaction with the Andromeda galaxy, which may influence their measured dynamical mass (de Rijcke et al. 2006). They may therefore be atypical examples of their class. We must look further afield for samples of dEs that are not tidally interacting with a larger galaxy. However beyond the Local Group, such galaxies are of low surface brightness making it very challenging for current telescopes to measure the internal motions of their stars.

The Local Group contains two dozen dSph galaxies. Although of lower luminosity than dEs, these dSph galaxies are sufficiently close to measure their velocity dispersions (from individual stars). They are all located within, or nearby to, the halos of the giant Milky Way and Andromeda galaxies. Many of them reveal an elongated asymmetric structure indicative of an ongoing tidal interaction.

Several different formation processes have been suggested for the origin of dE and dSph galaxies. These include: a) a *cosmological* origin in which the dwarfs are formed in the early universe. Although many will be accreted as the basic building blocks of larger galaxies, and some will merge with other dwarfs, a fraction of the original population may survive until today (Nagashima et al. 2005; Valcke et al. 2008; Bovill & Ricotti 2009); b) *environmental* processes that modify the structure of a larger progenitor galaxy. Here tidal interactions (Moore et al. 1996; Mastropietro et al. 2005; Mayer et al. 2007; D'Onghia et al. 2009) remove stellar and dark matter while so-called 'ram pressure' stripping can remove any gas (Penarubbia et al. 2008; Mayer et al. 2010); and c) gravitational collapse of dense *tidal* material that was left over from the collision of large galaxies (Okazaki & Taniguchi 2000). As dwarf galaxies appear to be a heterogeneous class of object, multiple origins may be required to explain their properties (see review by Lisker 2009).

The known UCDs are mostly located outside of the Local Group, in the Virgo, Fornax and Coma cluster of galaxies. They have similar *stellar* masses and luminosities to dSph galaxies but they are more compact. There is an ongoing debate as to whether UCDs were originally the nuclei of larger dwarf galaxies or are simply massive compact star clusters (Dabringhausen et al. 2008; Forbes et al. 2008; Mieske et al. 2008). In the former scenario, UCDs are the remnant of a nucleated dE galaxy that has lost its outer stars due to tidal stripping (Bekki et al. 2001), leaving only a nuclear star cluster which is subsequently identified as a UCD.

A key discriminant between the different origins for dwarfs is their predicted dark matter content. Cosmological models involving cold dark matter (DM) robustly predict high densities of DM at the centres of dwarf galaxies (e.g. Navarro et al. 2004). However the introduction of energy feedback from supernova explosions in hydrodynamical models, that incorporate stars and gas, show that gravitational heating causes the DM to expand to larger radii resulting in shallower DM profiles (Romano-Diaz et al. 2008; Mashchenko et al. 2008; Governato et al. 2010). These models can produce a dwarf galaxy with equal fractions of stars and DM within the effective radius. Simulations of galaxies that are subject to vigorous tidal and ram pressure stripping produce low mass, gas-free dE and dSph galaxies with a high DM fraction in their inner regions (Mayer et al. 2001). If dwarf galaxies had their origin in tidal material left over from a major collision then it is expected that they would be star-dominated, containing little or no dark matter (Okazaki & Taniguchi 2000). We note that the simulated tidal dwarf galaxy (model RS1-5) of Kroupa (1997) has an effective radius of 180 pc, velocity dispersion of 2.8 km s^{-1} and an inferred total-to-stellar mass of >100 (i.e. similar to the inferred properties of dSph galaxies) and yet it is DM-free. Simulations by Goerdt et al. (2008) suggest that a UCD formed by tidal stripping of a nucleated galaxy will be dark matter dominated. This is in contrast to the star cluster origin for UCDs in which they will be DM-free like globular clusters (Moore 1996; Lane et al. 2010; Conroy et al. 2010).

The abundances, luminosities and, particularly, the masses of dwarf galaxies can place a strong constraint on models of galaxy formation as dwarf galaxies are highly sensitive to the details of feedback processes (e.g. Benson et al. 2002) due to their shallow potential wells. This makes them a key population which any plausible model of galaxy formation must explain. The masses and DM content of dwarf galaxies in the gap ($-16 > M_K > -18$ mag), and hence the relative role of feedback and external environmental processes, is currently unknown. In particular, it is unknown if these galaxies will show a smooth transition in their dynamical properties from dEs to dSphs or to UCDs as we traverse from the high to the low mass side of the gap.

Here we present new measurements of the velocity dispersion of dE galaxies that lie within the gap using long exposures on the Keck 10 m telescope. With this data we derive their dynamical masses using the technique of Wolf et al. (2010) that is robust to the 3D orbits of the dynamical tracer stars. Our dynamical mass gives the total mass of stars, gas and dark matter within the 3D half light radius. It allows us to constrain the fraction of dark matter within a gap galaxy's inner regions and compare its properties to other dwarf systems for the first time.

2 SAMPLE SELECTION

We selected dwarf elliptical galaxies with K band magnitudes to lie within or close to the 'gap' reported by Forbes et al. (2008). These galaxies were further constrained to have no nucleus (dE) or only a small nuclear (dE,N) component as a nuclear cluster will have its own dynamical properties distinct from the underlying galaxy (Carter & Sadler 1990; Geha et al. 2002, 2003).

A total of five dwarf elliptical galaxies in the NGC 1407

Table 1. Dwarf Galaxy Sample Properties.

Galaxy Name	Type	Dist. (Mpc)	K (mag)	M_K (mag)	R_e ($''$)	R_e (pc)
LEDA 074886	dE	25	12.21	–19.79	∼9	1130
PGC 032348	dE,N	11	13.18	–17.04	11.9	638
VCC 1826	dE,N	16.5	13.50	–17.59	6.78	542
VCC 1407	dE,N	16.5	12.41	–18.68	11.27	902
VCC 846	E?	16.5	*	–17.84	12.74	1019

Notes: Galaxy types are from NED. Distance sources are LEDA 074886 (Trentham & Tully 2006), PGC 032348 (Trentham & Tully 2002) and VCC objects (Mei et al. 2007). K band magnitudes are from 2MASS (* no K band available, used M_g = –15.34 mag from Janz & Lisker 2009 and assumed g–K = 2.5. See Section 8.1 for details.). Geometric mean effective radii for the VCC galaxies are from Sérsic fits to surface brightness profiles from Janz & Lisker (2008), otherwise radii are measured in this work.

and Leo groups, and Virgo cluster were chosen for observation over a single night. The basic properties of the sample galaxies are listed in Table 1.

3 DATA ACQUISITION

The five dwarf elliptical galaxies were observed using the Echelle Spectrograph and Imager (ESI) on the Keck II 10m telescope on the night of 2010 January 10th. Conditions were clear with typical seeing for the science exposures of $0.8''$. Each galaxy was observed in high resolution (R ∼ 20,000) echelle mode giving a useful wavelength range of ∼4000 to 10,000 Å. The pixel scale varies from $0.12''$/pix in the blue to $0.17''$/pix in the red across the 10 echelle orders. The slit width was $0.5''$ giving an instrument resolution of $\sigma = 15.8$ km s^{-1} (although we can measure velocity dispersions of about half this value). The slit length is $20''$ and each galaxy was offset from the centre of the slit by about $5''$ giving increased radial coverage in one direction. Multiple exposures were taken of each galaxy, details of which are summarised in Table 2, along with seeing conditions and position angle of the slit. The position angles were chosen to match that of the galaxy major axis if available, otherwise parallactic angle was used. The approximate continuum signal-to-noise ratio in order 9 (∼ 8500Å) is also listed in Table 2. We also obtained spectra for a K giant with the same instrument settings as the science data.

Images in the B and R bands were also taken with ESI of the Leo group dwarf galaxy PGC 032348. The pixel scale for imaging is $0.15''$/pix. The total exposure times were 240 s in B and 120 s in R, with seeing conditions of $\sim 1''$. Digitized Sky Survey (DSS) images of the five galaxies and the slit positions are shown in Figure 1.

3.1 Data Reduction

After checking for consistency, individual calibration files such as bias frames, HgXe and CuAr arcs, internal flat fields were combined to create master files. The science frames, each of the same exposure time, were average combined in 2D using the IRAF software package. The individual science frames did not require shifting as the spatial alignment of the spectra was within 1 pixel from frame to frame. An average sigma clipping was used to reject cosmic rays.

Table 2. Observing Parameters.

Galaxy Name	Exp. time	Seeing	P.A.	S/N
LEDA 074886	20 × 7 = 140min	$0.75''$	103°	20
PGC 032348	25 × 4 = 100min	$0.80''$	65°	15
VCC 1826	20 × 3 = 60min	$0.75''$	-225°	25
VCC 1407	23 × 3 = 69min	$0.85''$	-225°	20
VCC 846	30 × 5 = 150min	$0.80''$	-208°	5

Notes: S/N is the typical signal-to-noise in the continuum at ∼8500Å.

Tracing and rectifying the spectra, wavelength calibration, extraction of 1D spectra in various apertures and background sky subtraction were all performed using the MAKEE program written by T. Barlow. The trace was carried out using a K giant standard star and gave residuals of $\leqslant 0.5$ pixel for orders 2–9 (orders 1 and 10 were not used in this analysis due to low signal). The background sky was taken from the edges of the slit, furthest from the galaxy centre. Although some faint background light from the galaxy may be contained in the sky apertures, there was no indication of the CaT absorption lines in the sky spectrum so this appears to be a very small effect.

4 SIZE MEASUREMENTS

Archival Subaru suprime-cam imaging of LEDA 074886 in the g band under $0.7''$ seeing conditions reveals an unresolved nucleus. Surrounding this is an elongated, disky structure (see Figure 2). The outer regions of the galaxy become very boxy. We modelled the galaxy isophotes using the IRAF task ellipse. This fitting process models each isophote with an ellipse that includes higher order Fourier components for boxyness and diskyness. However, it is not ideal for galaxies that are extremely disky, therefore our Sérsic profile fits to the 1D surface brightness profile should be regarded as somewhat tentative. We measure a Sérsic index n ∼ 1 and a geometric mean $R_e \sim 9''$. The nucleus contributes < 1% to the total galaxy luminosity. We note that these measurements are not used in the subsequent analysis as it appears from our imaging, and our spectral analysis below, that LEDA 074886 is not a pressure-supported dwarf elliptical galaxy (as is classified by Trentham & Tully 2006) but rather a late-type dwarf galaxy. We do however present the dynamical information for this galaxy here.

After reducing the ESI images of PGC 032348 using standard methods with IRAF software, the galaxy isophotes were fit with the IRAF task ellipse. A point-source plus Sérsic fit to the resulting B (R) band surface brightness profile gave n = 1.1 (1.2) and a geometric mean effective radius of $R_e = 11.9''$ ($11.4''$). The galaxy reveals an unresolved nucleus with a luminosity contribution of < 0.5% to the total galaxy light. An image of PGC 032348 and the B band surface brightness profile are shown in Figures 3 and 4.

The geometric mean R_e for the 3 Virgo cluster dEs are taken from Janz & Lisker (2008) who carried out Sérsic fits to the g band surface brightness profiles from SDSS images.

5 VELOCITY MEASUREMENTS

For PGC 032348 and VCC 846 the signal-to-noise of our spectra are such that we were only able to extract a single aperture that corresponds roughly to the FWHM size of the 2D galaxy spectrum. For the other three galaxies in the sample, we extracted a central aperture of ± 3 pixels ($0.9''$), which is on the order of the seeing. Additional independent apertures were also extracted either side of the galaxy centre. The size of the off-centre extraction apertures were designed to achieve a similar signal-to-noise ratio independent of radius. In Figure 5 we show the central aperture extraction centered around 8500Å for all five galaxies. This wavelength region includes the Calcium Triplet (CaT) lines which are used to obtain velocity and velocity dispersion measurements.

To obtain recession velocity and velocity dispersion measurements we selected stellar templates from two high-resolution stellar libraries (Montes et al. 1997 in the CaT region, and Bagnulo et al. 2008 in the Mg and Fe line region) covering a range of spectral types. These template stars were first broadened to the same spectral resolution as our data. We used the pPXF code of Cappellari & Emsellem (2004) to measure the first and second velocity moments of our galaxies (i.e., recession velocity and velocity dispersion). The pPXF routine simultaneously shifts, broadens and determines the best set of weighted template stellar spectra that minimises the residuals between the science spectrum and the fit. Spectral regions affected by strong skylines are manually excluded from the fit. This approach minimises errors due to template mismatch by allowing the simultaneous use of multiple possible templates (in our case typically a dozen per galaxy). It also allows for the fact that giant stars dominate the near-infrared (i.e. CaT region) whereas dwarf stars may have an increased contribution in the optical (i.e. Mg and Fe line region).

As an independent confirmation of our measurements we also ran pPXF using a *single* stellar spectrum taken on the same observing run with the same slitwidth as our galaxy spectra. The shifted and broadened stellar spectrum of this star (HR224) provided a good match to the Mg and Fe lines, and thus provides another measure of the velocity moments. The resulting velocity profiles are shown in Figures 6–8 with radii at the midpoint of the aperture.

For the three galaxies with off-nuclear apertures, a second order polynomial fit to the off-nuclear apertures was taken as representative of the galaxy velocity dispersion profile. The interpolated value at the galaxy centre is adopted as the galaxy central velocity dispersion, σ_0. The uncertainty in these measurements is assumed to be the full range of velocity dispersions from the Mg and Fe lines compared to those from the Ca Triplet lines.

For VCC 846 the velocity dispersion derived from using the stellar library varied from 14 to 24 km s^{-1}, whereas the stellar spectrum of HR224 gave 17 km s^{-1}. We adopt a central velocity dispersion of 19 ± 5 km s^{-1}. To further confirm this value, we attempted to measure the velocity dispersion with the Fourier cross-correlation method using the software package fxcor. This is somewhat more subjective than the pPXF method. We found a preferred value of 20 ± 10 km s^{-1}, i.e. consistent with our pPXF value.

For PGC 032348 we derived 13.8 and 17.0 km s^{-1} from the stellar library and 13.9 km s^{-1} using the ESI spectrum of HR224. We adopt a central velocity dispersion of 15.4 ± 1.6 km s^{-1} for PGC 032348.

Finally, we note that VCC 1407 was observed using ESI with a $0.75''$ slit by Evstigneeva et al. (2007). They extracted a single $1.5''$ aperture about the galaxy centre. From measurements of the Mg, Fe and Ca triplet regions they adopted a velocity dispersion of 30.4 ± 2.6 km s^{-1} over their aperture. A central velocity dispersion of 36 ± 5 km s^{-1} was derived from a medium resolution (R ∼ 5000) poor signal-to-noise spectrum by Chilingarian (2009). Our adopted central galaxy velocity is σ_0 = 25.5 ± 1.5 km s^{-1}.

The adopted central galaxy (σ_0) and nuclear aperture (σ_N) velocity dispersions for each galaxy are given in Table 3.

Table 3. Velocity Dispersion Measurements.

Galaxy Name	Nucleus σ_N (km s^{-1})	Galaxy σ_0 (km s^{-1})
LEDA 074886	24.1 ± 1.5	22.9 ± 0.6
PGC 032348	–	15.4 ± 1.6
VCC 1826	19.9 ± 0.5	22.3 ± 2.2
VCC 1407	23.7 ± 3.9	25.5 ± 1.5
VCC 846	–	19 ± 5

Notes: σ_N is the velocity dispersion measured at the nucleus, σ_0 is the velocity dispersion interpolated at the galaxy centre.

6 VELOCITY PROFILES

We have measured velocity profiles for three of our sample dE galaxies beyond the nucleus (see Figures 6–8). Two of the galaxies are dominated by random motions with no evidence for ordered rotation (although even at the largest radius probed our data are still within the effective radius). For the LEDA 074886 galaxy we find strong evidence of rotation, with a velocity of ∼ 30 km s^{-1} and $V/\sigma \geqslant 1$ (indicative of a disk) at the largest radii probed (∼ 0.5 R_e). Thus LEDA 074886 is not pressure-supported in its inner regions (we continue to list LEDA 074886 in the tables but it is not shown in subsequent figures). Our data are confined to the inner disk structure seen in the Subaru imaging (see Figue 2). The velocity dispersion profiles of all the galaxies show little or no trend with radius. Our interpolated galaxy central σ_0 values are all consistent with the nuclear value σ_N, indicating that the nucleus does not strongly affect the central kinematics in our sample galaxies (i.e. we see no evidence for central dips or peaks in the velocity dispersion).

7 INDIVIDUAL GALAXY NOTES

7.1 LEDA 074886

Classified as a non-nucleated dwarf elliptical, LEDA 074886 is a confirmed member of the NGC 1407 group with a recession velocity V = 1394 km s^{-1} (Brough et al. 2006). With M_K = –19.79 mag it is the highest luminosity galaxy in our sample. It may be interacting with the giant elliptical NGC 1407 (V = 1779 km s^{-1}) as it lies at a projected distance of only $8.4'$ or 61 kpc from its centre.

Table 4. Derived Properties.

Galaxy Name	M_{dyn} ($\times 10^8$ $M_\odot$)	M_* ($\times 10^8$ $M_\odot$)
LEDA 074886	5.5	19.7
PGC 032348	1.5	0.87
VCC 1826	2.5	1.5
VCC 1407	4.7	3.8
VCC 846	3.4	1.7

Notes: M_{dyn} is the dynamical mass within the 3D half light radius and M_* is the *total* stellar mass. See text for details.

Subaru suprime-cam imaging in $0.7''$ seeing indicates an elongated, disky structure in the galaxy central regions (see Figure 2). A small unresolved nucleus is seen at the galaxy centre. The galaxy bears a resemblance to the post tidal stripping model galaxy shown in figure 1 of Mayer et al. (2007).

Both the imaging and our velocity profiles suggest that the galaxy contains a thin embedded inner disk with ordered rotation. It is not a pressure-supported system in its inner regions and we exclude it from subsequent figures.

7.2 PGC 032348

This Leo group galaxy is listed as the dE,N galaxy CGCG 066-026 by Trentham & Tully (2002), who quote an R magnitude of 14.64. Our ESI imaging (see Figure 3) reveals an unresolved nucleus with a luminosity contribution of $< 0.5\%$.

7.3 VCC 1826

This Virgo dwarf galaxy was imaged as part of the ACS Virgo Cluster Survey. Sérsic fits to ACS images by Cote et al. (2006) give nuclear parameters of g = 20.12 and z = 18.91 for a small unresolved nucleus. The nucleus represents $< 2\%$ of the total galaxy flux. There is no nearby large galaxy.

7.4 VCC 1407

This Virgo dwarf galaxy was imaged as part of the ACS Virgo Cluster Survey. Sérsic fits to ACS images by Cote et al. (2006) give nuclear parameters of g = 20.40 and z = 19.40 for a nucleus of half light size = $0.127''$ (11.6 pc). The nucleus represents $< 2\%$ of the total galaxy flux. There is no nearby large galaxy.

7.5 VCC 846

VCC 846 is projected close to M87 but has a large blue shifted velocity of –730 km s^{-1} (NED). However the surface brightness fluctuation study of Jerjen et al. (2004) confirms its Virgo cluster membership. Barazza et al. (2003) list a B band $R_e = 12.35''$ and a Sérsic n value = 0.6. The Virgo spiral galaxy NGC 4402 lies at a projected distance of 31 kpc.

8 ADDITIONAL DATA SAMPLES

To supplement our data on low mass dE galaxies, we include literature data for other dwarf systems of similar mass. These include higher mass dEs and lower mass dwarf spheroidal galaxies and UCD objects (which may be galaxies or simply massive star clusters). All of these systems are pressure-supported in their inner regions, dominated by stars of old age, reveal smooth featureless morphologies and contain little or no gas (so that stellar masses are a good proxy for baryonic masses).

We note that the kinematic study of 73 galaxies by Simien & Prugniel (2002) includes some dwarf galaxies. The lowest luminosity with $M_B = -13.5$ mag ($M_K \sim -15.5$) and $\sigma_0 = 25 \pm 16$ km s^{-1} is UGC 5442, however it is classified as a late type Im galaxy. The lowest luminosity elliptical galaxy is PGC 39385 with $M_B = -14.48$ mag (and $M_K = -18.07$ mag from the 2MASS survey) and $\sigma_0 = 19 \pm 6$ km s^{-1}. Simien & Prugniel (2002) quote an effective radius for UGC 5442 but not PGC 39385. We have not used any data from the Simien & Prugniel (2002) study in this work.

8.1 Virgo cluster dwarf elliptical (dE) galaxies

The internal dynamics of 17 dE galaxies in the Virgo cluster were studied by Geha et al. (2002, 2003) using ESI on Keck. The main difference to our work is that they focused on brighter, more luminous dEs and they used a $0.75''$ slit (which has an effective resolution of 23.7 vs our 15.8 km s^{-1}). Their sample is also dominated by galaxies with nuclei, i.e. classified as dE,N.

They derive the average velocity dispersion for radii beyond $1''$ to avoid nuclear contamination. Their velocity dispersion profiles reveal central dips and peaks but are otherwise generally flat beyond $1''$. We take their value as a reasonable measure of the galaxy central velocity dispersion. As with our three Virgo dEs we take the R_e sizes from Janz & Lisker (2008).

K band photometry exists for 14/17 galaxies from the 2MASS survey. For the remaining 3 galaxies we take the g band magnitude from Janz & Lisker (2009) and apply a g–K = 2.5 transformation (equivalent to [Fe/H] = –1.3).

These data are supplemented by additional Virgo dE measurements from Chilingarian (2009). Here the off-nucleus velocity dispersions come from a variety of medium resolution (resolution ~ 50 km s^{-1}) spectra taken using different telescopes and instruments. Metallicities are also derived from the spectra. We use K band magnitudes from 2MASS and R_e sizes from Janz & Lisker (2008). We find that the Chilingarian data have a larger scatter for a given galaxy mass than the Geha et al. data. This is likely due to the poorer spectral resolution of the Chilingarian data.

As above, we assume a distance modulus to the Virgo cluster of m–M = 31.09.

8.2 Local Group dwarf spheriodal (dSph) galaxies

For the Milky Way satellite dSph galaxies we use the compilation of Wolf et al. (2010). From this we use their R_e size (in parsecs), velocity dispersions and V band luminosities. We note that the R_e sizes may not be directly comparable to those for dEs as they are often major axis values from

exponential fits to surface brightness profiles rather than geometric mean values from Sérsic law fits. In addition, velocity dispersions for dSph galaxies are generally measured from individual stars rather than integrated light. Metallicities for the individual dSph galaxies come from Kirby et al. (2009). For M31 dSph galaxies we use the recent studies of Kalari et al. (2010) and Collins et al. (2010) to obtain velocity dispersions, V band luminosities, R_e sizes (in parsecs) and metallicities.

8.3 Local Group dE galaxies

We take R_e sizes and the average galaxy velocity dispersions for the three Local Group peculiar dE galaxies (NGC 147, 185, and 205) from de Rijcke et al. (2006). Distance moduli and metallicities are assumed to be m–M = 24.43, 24.23 and 24.57 and [Fe/H] = –1.0, –1.2 and –0.9 for NGC 147, 185 and 205 respectively. We use K band magnitudes from the 2MASS LGA. We note that extinction corrected V band magnitudes from the RC3 would result in slightly lower stellar masses.

8.4 Ultra Compact Dwarfs (UCDs)

Here we adopt the working definition of a UCD as a compact ($R_e \leqslant 100$ pc) near-spherical object of mass greater than 2×10^6 $M_\odot$. This mass limit represents a (somewhat arbitrary) separation from lower mass GCs and corresponds to a relaxation timescale that is longer than the Hubble time (Dabringhausen et al. 2008). It also corresponds to the mass above which UCDs reveal a mass-metallicity and a size-mass relation that is not present in lower mass GCs (Forbes et al. 2008). Data for UCDs come from the homogeneous database of Mieske et al. (2008), which includes mostly Virgo and Fornax cluster objects. From this we take their R_e sizes, metallicities and their aperture-corrected velocity dispersions. Total K band magnitudes come from 2MASS where possible, otherwise the V band magnitude from the original source as listed by Mieske et al. (2008) is used. We have excluded the two very large, luminous objects (F-19 and VUCD7) for which the velocity dispersion is taken from the core while the effective radius and luminosity relate to the core plus halo (see also Evstingneeva et al. 2008).

9 MASS ESTIMATES

9.1 Stellar masses

Stellar masses are derived from K band magnitudes where possible and V band otherwise. The resulting luminosities are multiplied by a stellar mass-to-light (M/L) ratio, in the appropriate band, from a single stellar population model (Bruzual & Charlot 2003). The M/L varies with galaxy metallicity (or colour) for an assumed fixed mean age of 12 Gyrs and a Chabrier IMF. The advantage of working in the K band is that it is a good proxy for stellar mass with the M/L ratio being less sensitive to metallicity variations than optical bands. If the mean age of the stars were 5 Gyrs then the M/L ratios would be systematically lower by a factor of about 2, although for the systems studied here the stellar mass is dominated by old age stars. Variations due to different SSP models and IMFs have been explored by Dabringhausen et al. (2008). Thus from the total luminosity we derive the total stellar mass, listed in Table 4. To calculate the stellar mass within the effective radius we simply divide the *total* stellar mass by two. As these systems are largely devoid of gas, the stellar mass is equivalent to the baryonic mass.

9.2 Dynamical masses

Dynamical mass estimates of non-rotating, pressure-supported systems are typically obtained using the expression

$$M_{\rm dyn} = C\sigma^2 R, \tag{1}$$

where R is a measure of the size of the system and σ a measure of the system's velocity dispersion (Djorgovski, de Carvalho & Han 1988). The size of a system is often taken to be the effective, or half light, radius (R_e) which can be measured from a surface brightness profile. The observed σ, however, is often simply a central value. In principle, this can be corrected to a uniform standard (such as the total, luminosity-weighted, infinite-aperture, velocity dispersion) via the variable term C. This coefficient can allow for dynamical non-homology (e.g. a range of different velocity dispersion profile shapes).

The difference between some central aperture velocity dispersion measurement and the total aperture velocity dispersion is greater for the more highly concentrated systems which have high Sérsic indices and, through the Jeans equation (Ciotti 1991), also possess steeper aperture velocity dispersion profiles (Graham & Colless 1997, Simonneau & Prada 2004, Ciotti, Lanzoni & Renzini 1996, Busarello et al. 1997 and Prugniel & Simien 1997). Bertin et al. (2002) have calculated the value of C to be used with central velocity dispersions (within $1/8R_{\rm e}$) as a function of Sérsic index n, showing that C roughly equals 8, 4 and <2 when n equals 1, 4 and >10. While this variable term is needed, the long recognised problem is that these corrections are based on models having orbital isotropy (Ciotti & Lanzoni 1997; Mamon & Boué 2010). Large contributions from radial or tangential orbits will skew these mass estimates.

Recently, Wolf et al. (2010, their eq. 1) report that, independent of orbital anisotropy, the mass enclosed within a spherical volume of radius r_3 can be approximated by $3r_3\langle\sigma^2_{\rm total}\rangle/G$ when $\langle\sigma_{\rm total}\rangle$ is the luminosity-weighted, infinite-aperture, velocity dispersion and r_3 is the radius where the internal 3D density profile has a slope equal to -3. Given (i) the observation from Graham et al. (2006, their fig. 9) that the slope of density profiles is close to a value of -3 at their deprojected half light radii, coupled with (ii) Ciotti's (1991) finding that the deprojected half light radius is very close to 4/3 times the projected half light radius $R_{\rm e}$, then the mass can be approximated as $4R_{\rm e}\langle\sigma^2_{\rm total}\rangle/G$ (see also eq. 2 and Appendix B of Wolf et al.).

In this work we do not have total aperture velocity dispersions, but rather central aperture velocity dispersions (σ_0). However we note that the aperture velocity dispersion profiles of systems with Sérsic indices approximately less than 2 are expected to be flat (e.g. Graham & Colless 1997; Simonneau & Prada 2004). Indeed the velocity dispersion profile of the Local Group dEs NGC 147 and NGC 185

(Geha et al. 2010) is observed to be flat out to $1R_e$, and even to $5R_e$, using resolved star measurements. The UCDs, dSph and dEs examined here typically have Sérsic indices of $0.5 < n < 2$. We therefore use our central velocity dispersions as a proxy for the total, luminosity-weighted, aperture velocity dispersions.

In Table 4 we list the dynamical mass calculated using equation 1 with R_e as the size, σ_0 as the velocity dispersion and a coefficient of $C = 4$. This corresponds to the mass within a sphere containing half the system's light, rather than the entire system's mass. Dividing this mass by half of the galaxy's total light gives the mass-to-light ratio within the deprojected half light radius.

In passing we again note that a word of caution is warranted. We are able to use equation 1, with a constant C-term, to approximate the mass because we are dealing with dwarf systems which have flat velocity dispersion profiles. The velocity dispersion profiles of luminous elliptical galaxies, however, are not the same, instead being centrally-peaked. Consequently, the luminosity-weighted, infinite-aperture, velocity dispersion for these galaxies can be significantly different from the available (typically central) value. It is the former quantity which is required in equation 1 and obviously the use of a single coefficient in this equation cannot correct the central velocity dispersion for all of these varying differences. For this reason Wolf et al. (2010) note that this equation approximates the mass "under the assumption that the observed [luminosity-weighted] stellar velocity dispersion profile is relatively flat near [and beyond] R_e", and that one actually uses the luminosity-weighted, velocity dispersion within R_e in this equation. Any mass or Fundamental Plane analysis including luminous elliptical galaxies will introduce a systematic bias with mass if central velocity dispersions are used together with a constant coefficient in equation 1. One method of compensating for this is to adopt a variable coefficient, as tabulated by Bertin et al. (2002).

10 RESULTS AND DISCUSSION

In Figure 9 we show our new velocity dispersion measurements vs the derived dynamical mass within the half light radius for our four dE galaxies plus other pressure-supported dwarf systems. We also highlight the mass gap ($8 \times 10^7 < M_{dyn}/M_\odot < 5 \times 10^8$) defined to lie between the lowest mass dEs beyond the Local Group and the highest mass dSph galaxies. As well as two peculiar Local Group dE galaxies (NGC 147 and NGC 185), the gap now includes three more dE galaxies (the Leo group galaxy PGC 032348, and the Virgo cluster galaxies VCC 1826 and VCC 846). The two peculiar dEs from the Local Group hint at a connection with UCDs, however the addition of the three new dEs strongly indicates a continuous trend of a declining velocity dispersion with declining dynamical mass, from dEs to the lower mass dSph galaxies. The slope of the relation ($M_{dyn} \sim \sigma^{2-3}$) is similar to that found by others for dEs and dSph galaxies when luminosity (stellar mass) is considered (e.g. de Rijcke et al. 2005).

Figure 10 shows the effective radius in parsecs as a function of the dynamical mass within the half light radius. The galaxies in the mass gap have effective radii that are comparable to the most massive dSph galaxies. Thus a continuity exists, albeit with a change in slope (Graham et al. 2006; Graham & Worley 2008; Misgeld et al. 2009), between the effective sizes of dSph and dE galaxies over a range of greater than one thousand in mass. We note that such continuous trends are now recognised to extend all the way from dEs to giant ellipticals (Graham & Guzman 2003; Cote et al. 2006; Misgeld et al. 2009).

The UCDs have sizes that are on average about one tenth those of dSph galaxies. We note that the size-mass trend for UCDs is consistent with models by Murray (2009) that describe optically thick star clusters without dark matter. This provides further support for the claims that UCDs are simply massive star clusters.

The continuous trends of decreasing velocity dispersion and effective radius with decreasing mass from dEs to dSph galaxies (Figures 9 and 10), are qualitatively similar to the model predictions for an early cosmological origin for dwarf galaxies of Nagashima et al. (2005) and Valcke et al. (2008). In Figures 9 and 10 we overplot the 'C' models from Table 3 of Valcke et al. which represent the final (after 10 Gyr) properties of their model galaxies. We calculate the dynamical mass of their model galaxies using equation 1. The models have a similar trend to the data but are offset in both velocity dispersion and effective radius. A key ingredient in dwarf galaxy formation models is the degree of energy feedback from supernovae which determines the depth of the potential well (Mashchenko et al. 2008). Strong feedback will result in a more diffuse DM halo which has a smaller central velocity dispersion and more extended stellar profile. As noted by Valcke et al. (2008) *"The combination of R_e and central σ [velocity dispersion] thus provide an excellent tool to evaluate the soundness of halo properties within a certain framework of galaxy formation."*

As most pressure-supported dwarf systems are devoid of gas, the dynamical mass we derive is essentially equal to the mass in stars plus dark matter. In Figure 11 we show the ratio of the dynamical mass to the stellar mass within the half light radius. This ratio is equivalent to a mass-to-light ratio once the effects of stellar metallicity have been removed. A ratio of unity indicates that the dynamical mass equals the stellar mass within the effective radius, so no dark matter (DM) is required. The UCDs reveal a slightly elevated ratio. This may indicate the presence of some dark matter or be simply due to a non-standard IMF that is not accounted for in current stellar population models (for more discussion see Dabringhausen et al. 2008; Mieske et al. 2008; Forbes etal. 2008). We note that a change to a more top-heavy IMF with increasing total mass is expected in the optically-thick star cluster model of Murray (2009). The gap galaxies reveal little, or no, evidence for DM in their inner regions. This is in stark contrast to the dSph galaxies which show a rapidly rising ratio (indicative of more DM) for dynamical masses less than 8×10^7 $M_\odot$. Thus the gap galaxies are star-dominated like higher mass dE galaxies and do not reveal an increase in their dynamical-to-stellar mass ratio as seen for the DM dominated dSph galaxies. The gap galaxies may represent a local minimum in the inner region DM fraction for dwarf galaxies in which the process of gravitational heating of the DM from stellar feedback is at its most efficient.

This paper, like Forbes et al. (2008), Dabringhausen et al. (2008) and Mieske et al. (2008), has used three

basic quantities: velocity dispersion, size, and luminosity. Through the luminosity expression $L = 2\Pi\langle I\rangle_{\rm e} R_{\rm e}^2$, involving the mean intensity $\langle I\rangle_{\rm e}$ inside the half-light radius $R_{\rm e}$, our work is in essence a variation of Fundamental Plane studies (Djorgovski & Davis 1987). Throughout the 1990s it was generally thought that galaxies with velocity dispersions less than ∼100 km s^{-1}, and thus our dwarf galaxies, were not connected with bright elliptical galaxies because they did not follow the same two-dimensional plane in three-dimensional spaces that used these quantities. Moreover, Bender, Burstein & Faber (1992) had shown that dEs and Es resided in disconnected regions of this three parameter space. However, it is now understood that this apparent disconnection was a result of sample selection which missed the bridging population, and Graham & Guzmaán (2004) and Graham (2005) have since advocated that the two populations are actually united through a continuous curved distribution of points, noting that the "Fundamental Plane is simply the tangent sheet to the highluminosity end of a curved surface". A variant of this manifold was parameterised by Zaritsky et al. (2006, 2008), who referred to it as the "Fundamental Manifold", to which they added disc galaxies, galaxy clusters and dwarf spheroidal galaxies, and globular clusters (Zaritsky et al. 2010). The potentially unifying and curved nature of this surface is receiving renewed interest, although collectively we still need to be careful to account for systematic, mass-dependent variations in galaxy structure and dynamics. The use of a constant C-term and central velocity dispersions when dealing with giant elliptical galaxies will mis-shape the true surface, and thus one's conclusions about how the mass-to-light ratio varies across the surface.

In Figure 12 we show the 3D manifold of effective radius, dynamical mass and stellar mass for dwarf systems. This can be compared to the recent 3D manifold of radius, dynamical mass and luminosity presented by Tollerud et al. (2010). Like Tollerud et al., we conclude that UCDs do not follow the general trend seen for dEs and dSph galaxies. Tollerud et al. also discuss the manifold of Zaritsky et al. (2010) that includes GCs and UCDs, as well as dSph and elliptical galaxies. Tollerud et al. present a 3D figure that includes the 'warped' manifold of Zaritsky et al. showing how this can incorporate GCs and UCDs. However, GCs and UCDs occupy a different part of the manifold to dSph galaxies without any bridging population with intermediate properties. In other words, a bifurcation exists at these mass scales, with UCDs and dSph galaxies occupying different branches. This is consistent with our findings of a different evolutionary history.

Although dE and dSph galaxies form continuous trends in Figures 9 and 10, the dynamical-to-stellar mass ratio trend seen in Figure 11 suggests a dramatic change in slope (and DM content) for masses lower than the mass gap. This can be understood in the context of their local environment. All of the dSph galaxies examined here are located within, or near, the halo of a giant galaxy, namely the Milky Way or Andromeda. Whereas the dE galaxies are located in groups or clusters and not necessarily within the halo of a massive galaxy. Thus the evolutionary history of the Local Group dSph galaxies may have been different from dwarfs of similar mass that are not subject to the same degree of star and gas removal. The extent of this mass loss due to stripping depends on the mass, and mass density, of the progenitor galaxy, as well as the strength of the tidal interaction, and the efficiency of forming stars from any gas before it is stripped away (Mayer et al. 2001). These parameters may in turn depend on the epoch of formation of the dwarf galaxy and when it is accreted into a larger halo (Maccio, Kang & Moore 2009). Thus, depending on the exact processes and timescales, a range of dynamical-to-stellar mass ratios for dwarf galaxies might be expected.

Simulations of tidal 'harassment' in a Virgo cluster-like potential (Mastropietro et al. 2005) indicate that some galaxies can lose a significant fraction of their DM without much star loss, so that the remnant dwarf galaxy is dominated by stars in its inner region as we have found for the gap galaxies. An alternative possibility is that these low mass dE galaxies were formed with little central DM. The gap galaxies may represent the first indications of a population of even lower mass dE galaxies that have similar dynamical masses to Local Group dSph galaxies but are star-dominated in their inner regions due to their location outside of a giant galaxy halo. Dynamical studies of samples of low mass dwarf galaxies, beyond the Local Group, with the next generation of large telescopes will be able to test this suggestion.

11 CONCLUSIONS

Using the ESI instrument on the Keck telescope we have obtained internal kinematics for four dwarf ellipticals and one late-type dwarf galaxy. These galaxies were selected to have little, or no, nuclear component and indeed there is no evidence for a significant kinematically distinct nucleus in our data. The galaxies have K band magnitudes down to $M_K \sim -17$ mag which places them in the 'gap' between previous dynamical mass measurements of dE galaxies by Geha et al. (2003) and Chilingarian (2009) and Local Group dwarf spheriodal (dSph) galaxies and Ultra Compact Dwarf (UCD) objects located in the Virgo and Fornax clusters. We define the dynamical mass gap to be between $8 \times 10^7 < M_{dyn}/M_\odot < 5 \times 10^8$.

We measure central velocity dispersions of around 20 km s^{-1} for each galaxy. Supplemented by data from the literature for dE, dSph and UCD objects, we derive total stellar masses (mostly from K band magnitudes) and dynamical masses (using the formulation of Wolf et al. 2010).

We find that the dE galaxies in the mass gap suggest a continuity from dE to dSph galaxies in terms of both their central velocity dispersion and effective radius with dynamical mass. This is also true when these systems are examined in the 3D space of radius, dynamical mass and stellar mass. Such trends are qualitatively similar to those expected for dwarf galaxies from cosmological formation models. Interestingly, the dE galaxies in the gap reveal dynamical-to-stellar mass ratios, within their half light radii, of unity. Thus they appear to be stellar-dominated in their inner regions similar to higher mass dE galaxies and do not reveal the need for large dark matter fractions as inferred for Local Group dSph galaxies. We speculate that any dark matter in the inner regions of these low mass dE galaxies has been 'puffed-up' to larger radii by gravitational heating effects from supernova feedback. Probing the dynamics of even lower mass dEs may

reveal a population of dwarf galaxies that are dominated by stars in their inner regions.

12 ACKNOWLEDGEMENTS

We thank J. Janz and T. Lisker for supplying their Virgo cluster dE data in machine readable form. We thank E. Tollerud and J. Wolf for useful discussions on galaxy scaling relations. This project made use of the NASA Extragalactic Database (NED) and data products from the Two Micron All Sky Survey, which is a joint project of the University of Massachusetts and the Infrared Processing and Analysis Center/California Institute of Technology, funded by the National Aeronautics and Space Administration and the National Science Foundation. We thank the staff of the W. M. Keck Observatory for their support. Some the data presented herein were obtained at the W.M. Keck Observatory, which is operated as a scientific partnership among the California Institute of Technology, the University of California and the National Aeronautics and Space Administration. We acknowledge financial support from the Access to Major Research Facilities Programme which is a component of the International Science Linkages Programme established under the Australian Government's innovation statement, Backing Australia's Ability.

13 REFERENCES

Barazza, F. D., Binggeli, B., Jerjen, H., 2003, A&A, **407,** 121
Bagnulo, S., et al., 2008, The ESO Messenger, **114,** 10
Bekki, K., Couch, W. J., Drinkwater, M. J., 2001, ApJ, **552,** L105
Bender, R., Burstein, D., Faber, S., 1992, ApJ, 399, 462
Benson, A., Frenk, C., Lacey, C., Baugh, C., Cole, S., 2002, MNRAS, 333, 177
Benson, A. J., Bower, R., 2010, MNRAS, **405,** 1573
Bertin, G., Ciotti, L., Del Principe, M., 2002, A&A, 386, 149
Bovill, M. S., Ricotti, M., 2009, ApJ, **693,** 1859
Brough, S., Forbes, D. A., Kilborn, V. A., Couch, W., Colless, M., 2006, MNRAS, **369,** 1351
Bruzual, G., Charlot, S., 2003, MNRAS, **344,** 1000
Busarello, G., Capaccioli M., Capozziello S., Longo G., Puddu E., 1997, A&A, 320, 415
Cappellari, M., Emsellem, E., 2004, PASP, **116,** 138
Carter, D., Sadler, E., 1990, MNRAS, 245, 12
Chilingarian, I. V., 2009, MNRAS, **394,** 1229
Ciotti, L., 1991, A&A, 249, 99
Ciotti, L., Lanzoni B., 1997, A&A, 321, 724
Ciotti, L., Lanzoni B., Renzini A., 1996, MNRAS, 282, 1
Collins, M. L. M., et al. 2010, arXiv:0911.1365
Conroy, C., Loeb, A., Spergel, D., 2010, ApJ, in press
Côté, P., et al. 2006, ApJSS, **165,** 57
Dabringhausen, J., Hilker, M., Kroupa, P., 2008, MNRAS, **386,** 864
De Rijcke, S., Prugniel, P., Simien, F., Dejonghe, H., 2006, MNRAS, **369,** 1321
Djorgovski, S., de Carvalho, R., Han, M., 1998, ASPC, 4, 329
D'Onghia, E., Besla, G., Cox, T. J., Hernquist, L., 2009, *Nature,* **460,** 605
Evstigneeva, E. A., Gregg, M. D., Drinkwater, M. J., Hilker, M., 2007, **133,** 1722
Evstigneeva, E. A., Drinkwater, M. J., Peng, C. Y., Hilker, M., De Propris, R., Jones, J. B., Phillipps, S., Gregg, M. D., Karick, A. M., 2008, AJ, **136,** 461
Forbes, D., et al., 2008, MNRAS, **389,** 1924
Geha, M., Guhathakurta, P., van der Marel, R. P., 2002, AJ, **124,** 3073
Geha, M., Guhathakurta, P., van der Marel, R. P., 2003, AJ, **126,** 1794
Goerdt, T., Moore, B., Kazantzidis, S., Kaufmann, T., Macciò, A. V., Stadel, J. 2008. MNRAS, **385,** 2136
Governato, F., et al. 2010, *Nature,* **463,** 203
Graham, A., Colless M., 1997, MNRAS, 287, 221
Graham, A., Guzman, R., 2003, AJ, 125, 2936
Graham, A., Guzman, R., 2004, in Penetrating bars through masks of cosmic dust, ed. D. Block et al., Kluwer Academic Publishers.
Graham, A., 2005, in Near-field Cosmology with Dwarf Elliptical Galaxies, ed. H. Jerjen and B. Binggeli, IAU 198.
Graham, A., Merritt D., Moore B., Diemand J., Terzić B., 2006, AJ, 132, 2711
Graham, A., Worley, C. C., MNRAS, **388,** 1708
Janz, J., Lisker, T., 2008, ApJ, **689,** L25
Janz, J., Lisker, T., 2009, ApJ, **696,** L102
Jerjen, H., Binggeli, B., Barazza, F. D., 2004, AJ, **127,** 771
Kalirai, J. S., Beaton, R. L., Geha, M. C., Gilbert, K. M., Guhathakurta, P., Kirby, E. N., Majewski, S. R., Ostheimer, J. C., Patterson, R. J., Wolf, J., 2010, ApJ, **711,** 671
Kirby, E. N., Guhathakurta, P., Bolte, M., Sneden, C., Geha, M. C., 2009, ApJ, **705,** 328
Kroupa, P., 1997, *New Astronomy,* **2,** 139
Lane, R. et al. 2010, MNRAS, in press
Lisker, T., 2009, AN, **330,** 1403
Macciò, A. V., Kang, X., Moore, B. 2009, ApJ, **692,** L109
Mamon, G. A., Boué, G., 2010, MNRAS, 401, 2433
Mashchenko, S., Wadsley, J., Couchman, H. M. P., 2008, *Science,* 319, 174
Mastropietro, C., Moore, B., Mayer, L., Debattista, V. P., Piffaretti, R., Stadel, J. 2005, MNRAS, **364,** 607
Mayer, L., Governato, F., Colpi, M., Moore, B., Quinn, T., Wadsley, J., Stadel, J., Lake, G., 2001, ApJ, **559,** 754
Mei, S., Blakeslee, J. P., Côté, P., Tonry, J. L., West, M. J., Ferrarese, L., Jordán, A., Peng, E. W., Anthony, A., Merritt, D., 2007, ApJ, **655,** 144
Mieske, S., et al. 2008, A&A, **487,** 921
Misgeld, I., Hilker, M., Mieske, S., 2009, A&A, **496,** 683
Montes, D., Martin, E. L., Fernandez-Figueroa, M. J., Cornide, M., de Castro, E., 1997, A&AS, 123, 473
A&ASS, **123,** 473
Moore, B., Katz, N., Lake, G., Dressler, A. & Oemler, A., 1996, *Nature,* **379,** 613
Moore, B., 1996, ApJ, **461,** L13.
Murray, N., 2009, ApJ, **691,** 946
Nagashima, M., Yahagi, H., Enoki, M., Yoshii, Y., Gouda, N. 2005, ApJ, **634,** 26
Navarro, J. F., Frenk, C. S., White, S. D. M., 1997, ApJ, **490,** 493
Okazaki, T., Taniguchi, Y., 2000, ApJ, **543,** 149
Peñarrubia, J., Navarro, J. F., McConnachie, A. W. 2008.

ApJ, **673,** 226
Proctor, R., Philip, L., Forbes, D., Colles, M., Couch, W., 2008, MNRAS, 386, 1781
Prugniel, P., Simien F., 1997, A&A, 321, 111
Romano-Diaz, E., Shlosman, I., Hoffman, Y., Heller, C., 2008, ApJ, 685, 105
Simonneau, E., & Prada, F. 2004, RMXAA, 40, 69
Simien, F., Prugniel, Ph., 2002, A&A, 384, 371
Tollerud, E., Bullock, J., Graves, G., Wolf, J., 2010, arXiv:1007.5311
Toloba, E., et al., A&A, in press
Trentham, N., Tully, R. B., Mahdavi, A., 2006, MNRAS, **369,** 1375
Trentham, N., Tully, R. B., 2002, MNRAS, **335,** 712
Valcke, S., de Rijcke, S., Dejonghe, H., MNRAS, **389,** 1111
Wolf, J. et al. 2010, MNRAS, **406,** 1220
Zaritsky, D., Gonzalez, A., Zabludoff, A., 2006, ApJ, 638, 725
Zaritsky, D., Zabludoff, A., Gonzalez, A., 2010, arXiv:1011.4945

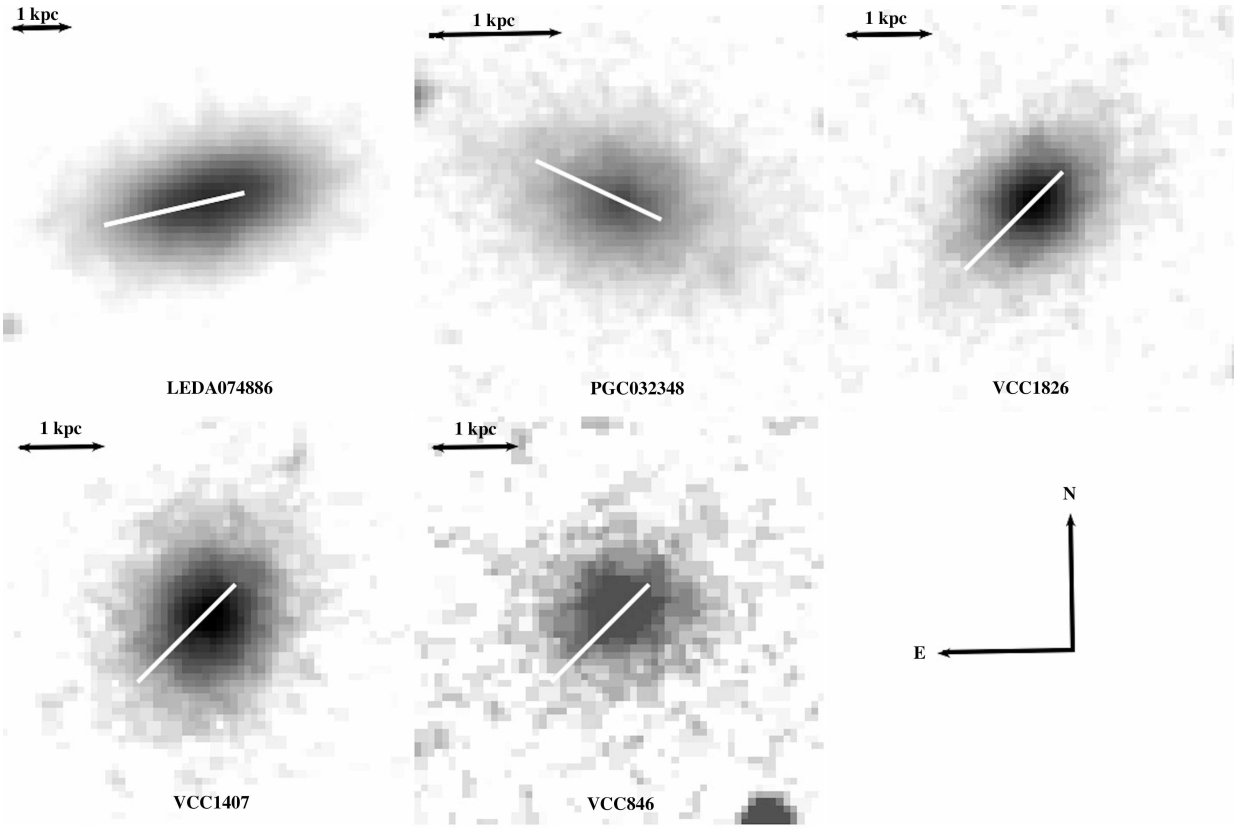

Figure 1. Montage of the dwarf galaxy sample. The orientation and length of the ESI slit is shown on images from the Digitized Sky Survey. North is up and East is left. A 1 kpc scale bar is shown in each image.

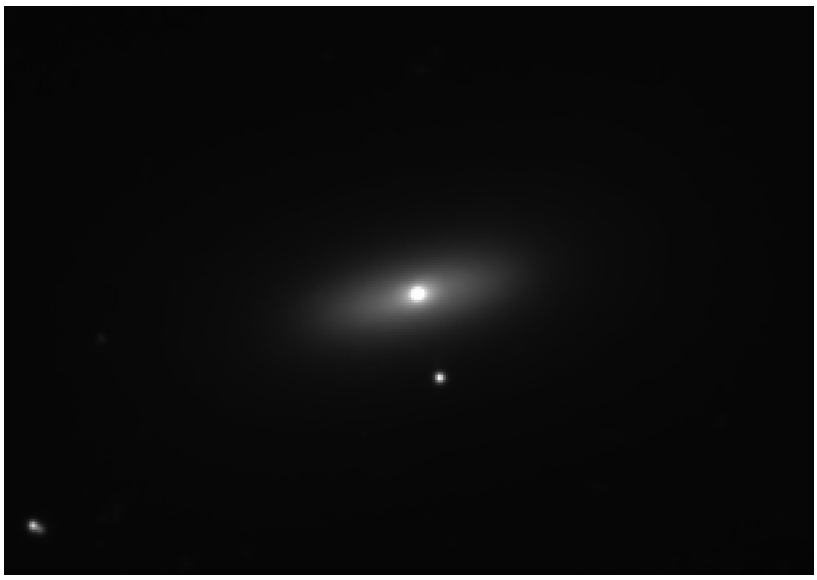

Figure 2. Image of LEDA 074886. The image size is approximately $60'' \times 45''$. North is up and East is left. At the distance of LEDA 074886, $1''$ equals 120 pc. The central nucleus and inner elongated disk structure is clearly seen.

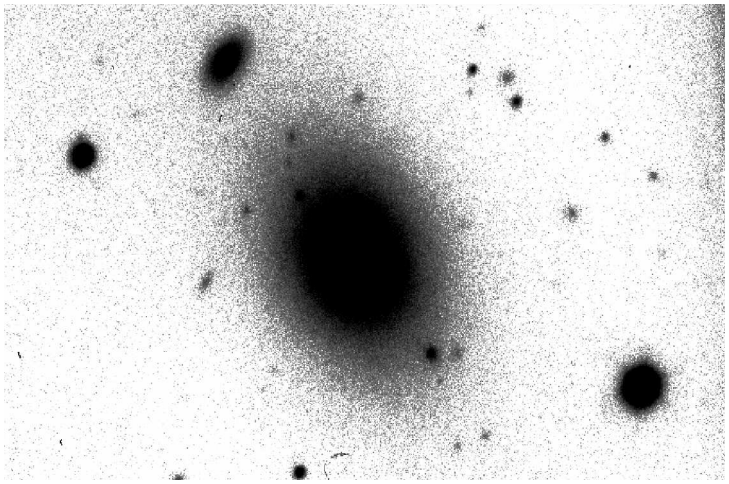

Figure 3. Negative image of PGC 032348. The image size is $105'' \times 70''$. North is up and East is left. At the distance of PGC 032348, $1''$ equals 53 pc.

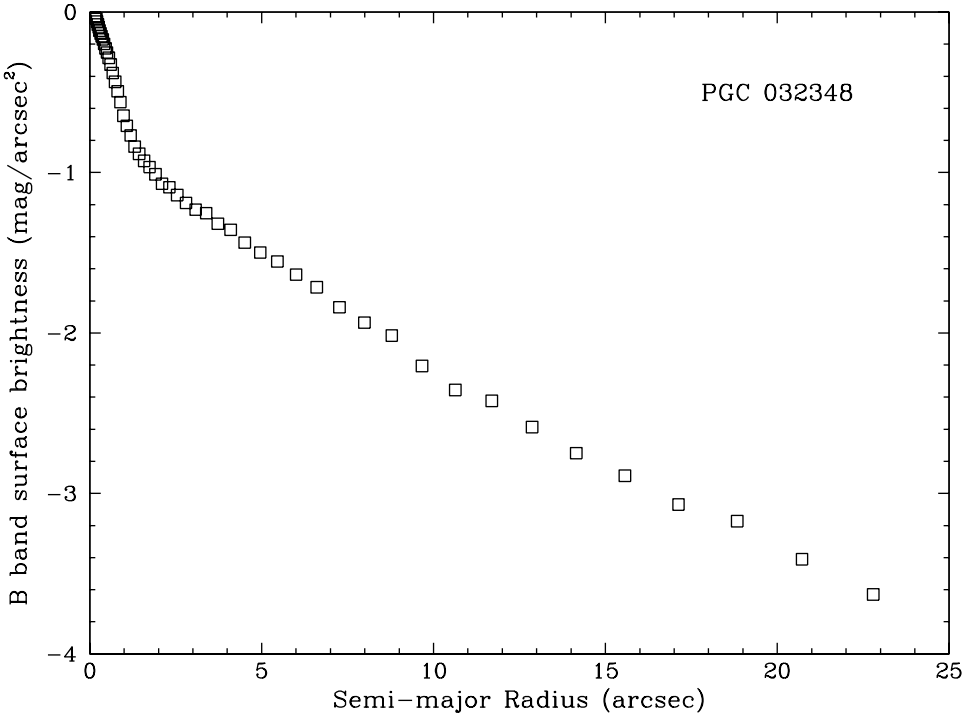

Figure 4. B band surface brightness profile of PGC 032348. The surface brightness has been normalised to the galaxy centre.

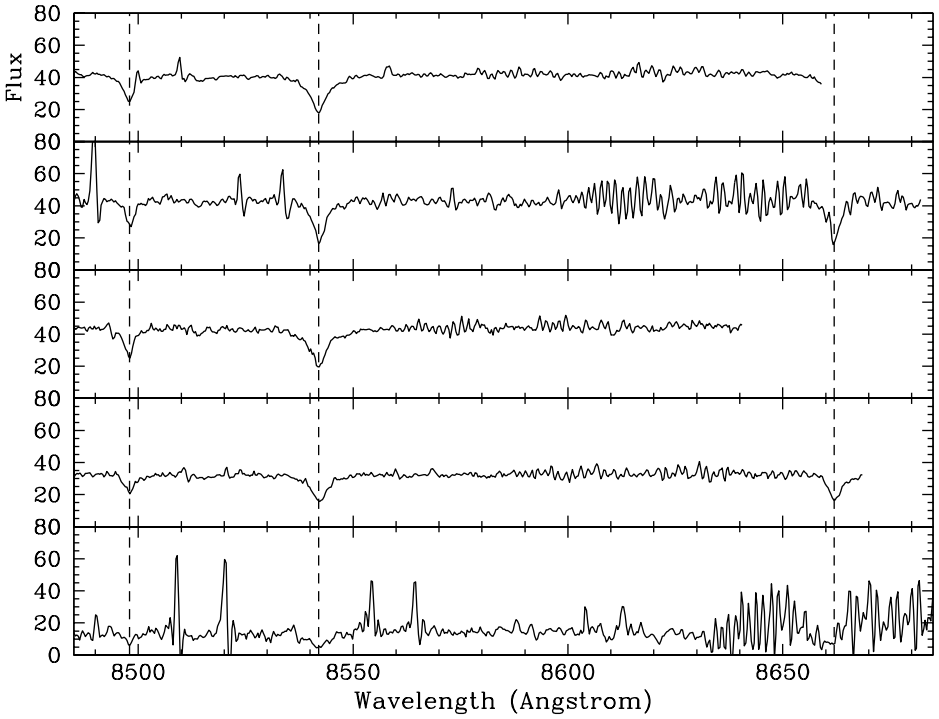

Figure 5. ESI spectra of dwarf galaxies. Top to bottom are LEDA 074886, PGC 03248, VCC 1826, VCC 1407 and VCC 846. The rest wavelength spectra show the central aperture extraction for each dwarf galaxy. The three Calcium Triplet lines (8498, 8542, 8662Å) are indicated by dashed lines. Regions affected by skylines are excluded from the spectral fits. For some spectra only two of the three CaT lines are available.

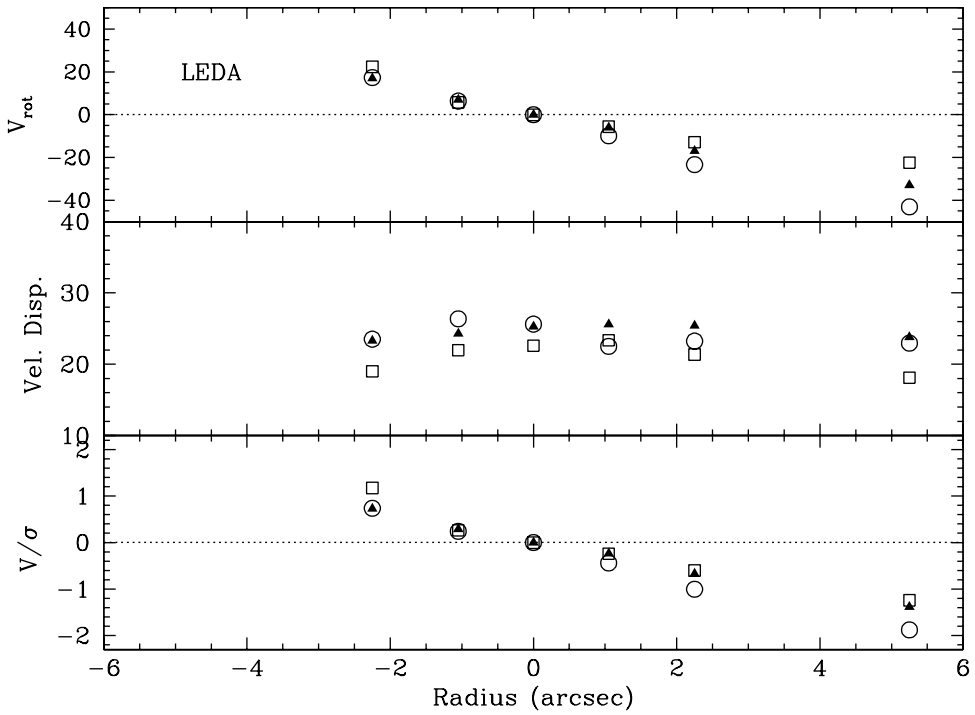

Figure 6. Velocity profile for LEDA 074886. *Top* panel shows the rotation velocity (normalised to the galaxy systemic velocity at the galaxy centre). *Middle* panel shows the velocity dispersion. *Lower* panel shows the V/σ ratio (normalised to zero at the galaxy centre). The symbols show the results from the stellar library fit to the Mg and Fe region (open squares), the Ca Triplet region (open circles) and from the ESI template star to the Mg and Fe region (filled triangles).

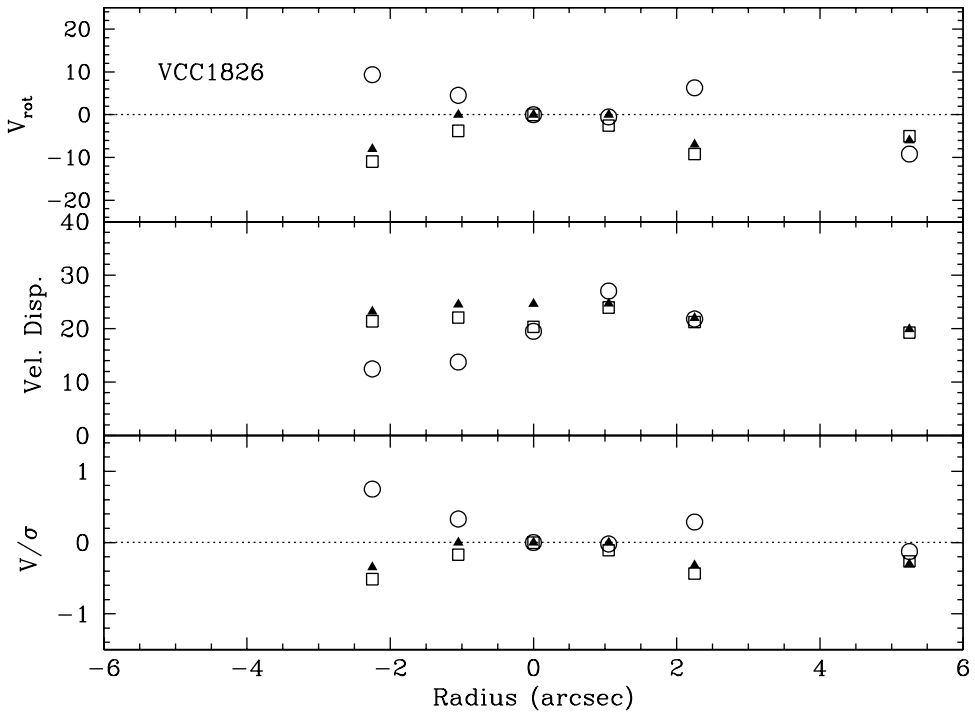

Figure 7. Velocity profile for VCC 1826. *Top* panel shows the rotation velocity (normalised to the galaxy systemic velocity at the galaxy centre). *Middle* panel shows the velocity dispersion. *Lower* panel shows the V/σ ratio (normalised to zero at the galaxy centre). The symbols show the results from the stellar library fit to the Mg and Fe region (open squares), the Ca Triplet region (open circles) and from the ESI template star to the Mg and Fe region (filled triangles).

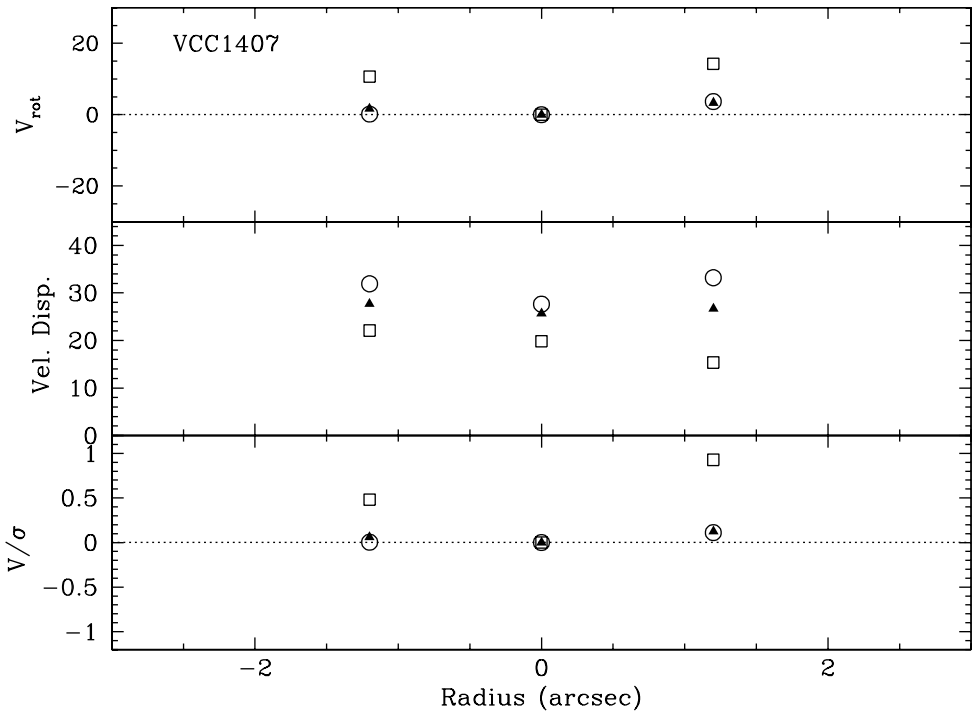

Figure 8. Velocity profile for VCC 1407. *Top* panel shows the rotation velocity (normalised to the galaxy systemic velocity at the galaxy centre). *Middle* panel shows the velocity dispersion. *Lower* panel shows the V/σ ratio (normalised to zero at the galaxy centre). The symbols show the results from the stellar library fit to the Mg and Fe region (open squares), the Ca Triplet region (open circles) and from the ESI template star to the Mg and Fe region (filled triangles).

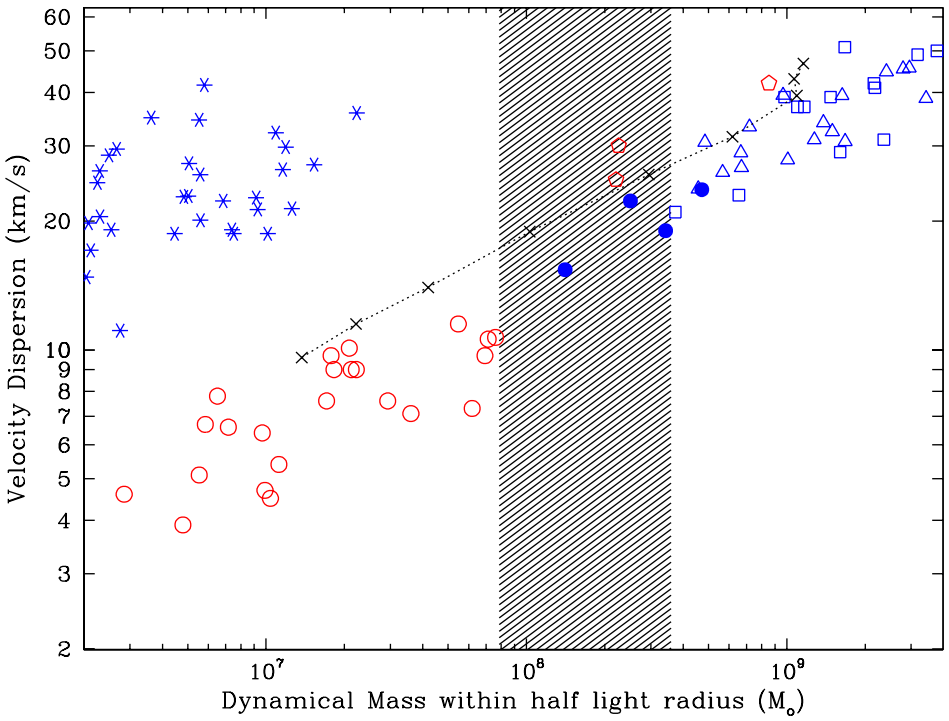

Figure 9. Dwarf galaxy velocity dispersion vs dynamical mass within the deprojected half light radius (equal to 4/3 R_e). Symbols are as follows: red for dwarfs located in the Local Group and blue for external dwarfs, with open circles for Milky Way and M31 dwarf spheroidal (dSph) galaxies (Wolf et al. 2010) and open pentagons for Local Group dwarf elliptical (dE) galaxies (NGC 147, 185 and 205; de Rijcke et al. 2006) and stars for ultra compact dwarfs (UCDs; Mieske et al. 2008), open triangles (Chilingarian 2009) and squares (Geha et al. 2003) for Virgo dE galaxies. Our new data is shown by filled blue circles. The dynamical mass is calculated using the technique of Wolf et al. (2010) which has the advantage of being robust to the actual 3D orbits of the dynamical tracer stars. The shaded region shows the dynamical mass gap between external dE galaxies and dSph galaxies. The dotted lines and crosses show the N-body/SPH models of dwarf galaxies from Valcke et al. (2008). Our new data suggest a continuous trend in velocity dispersion from dE galaxies to the lower mass dSph galaxies, rather than the UCDs.

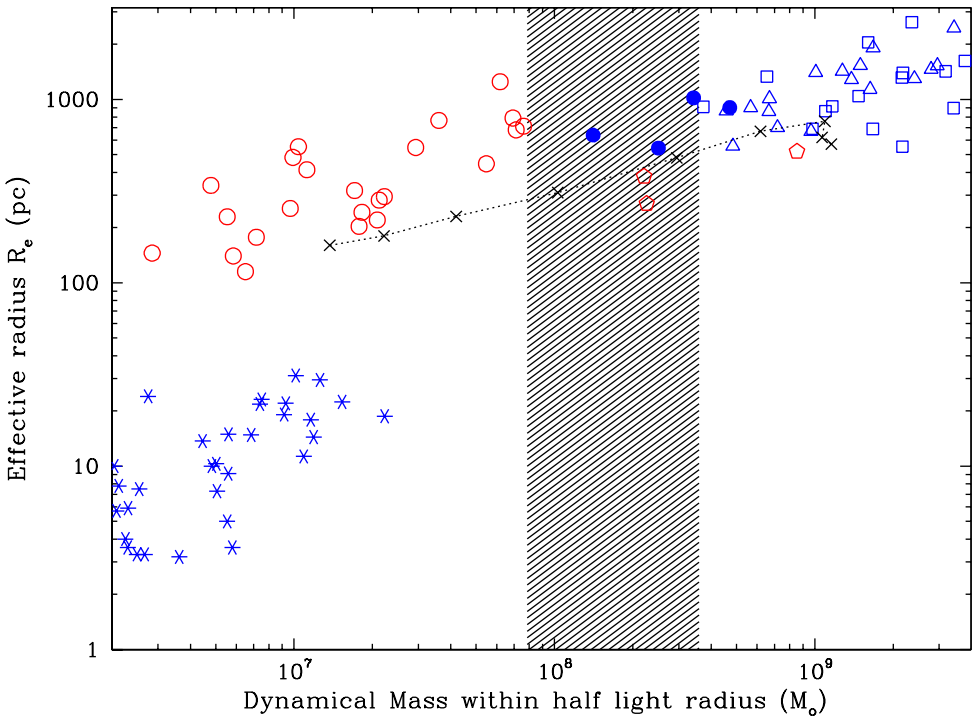

Figure 10. Dwarf galaxy effective radius (R_e) vs dynamical mass. Same symbols as Figure 9. The dotted lines and crosses show the N-body/SPH models of dwarf galaxies from Valcke et al. (2008). Although a slight change of slope is apparent, the new data again indicate a continuous trend from dE to lower mass dSph galaxies.

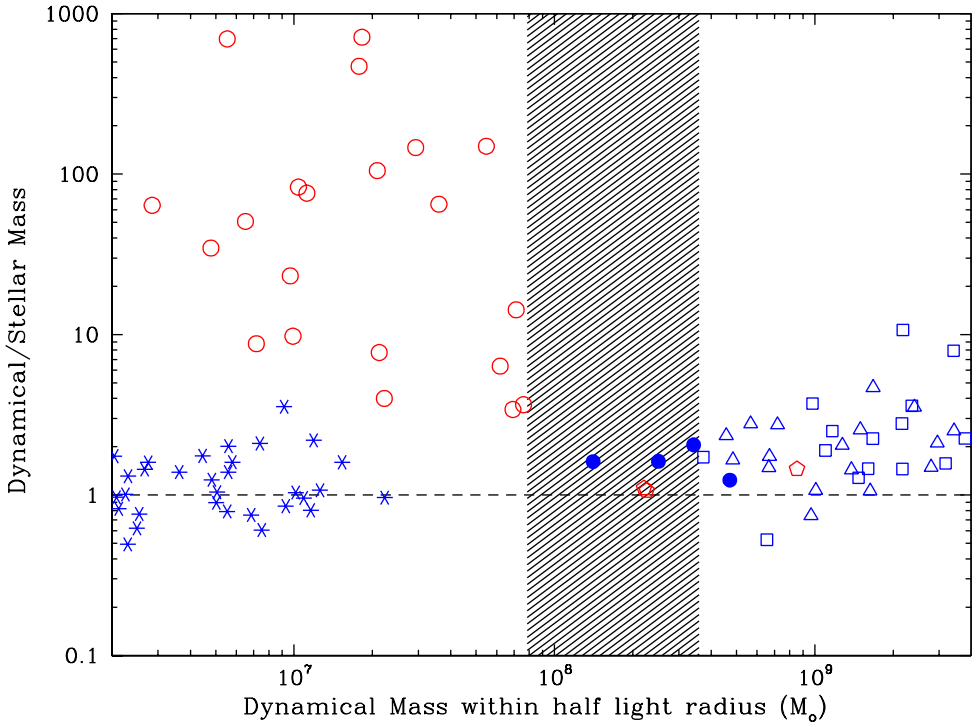

Figure 11. The ratio of dynamical-to-stellar mass vs dynamical mass for dwarf galaxies. Same symbols as Figure 9. The stellar mass is calculated from an observed total luminosity times a mass-to-light ratio (in the appropriate photometric band) that depends on metallicity from stellar population models (Bruzual & Charlot 2003). We assume a fixed age of 12 Gyrs as dwarfs tend to be dominated by old age stars. This total stellar mass is then divided by two to give the stellar mass within the half light radius. A ratio of unity, shown by the dashed line, indicates when the dynamical mass equals the stellar mass. The UCD objects scatter about a value of unity, consistent with them being dark matter free star clusters. Both the Local Group dE galaxies (NGC 147 and 185) and the new data indicate that there is little, or no, evidence for dark matter in mass 'gap' galaxies in their inner regions. The dSph galaxies show a rapidly rising ratio (indicative of more dark matter) for dynamical masses less than 8×10^7 $M_\odot$. There is also a hint of an upturn for the most massive dE galaxies suggesting that dark matter may start to play a role within their inner regions. The gap galaxies are star-dominated like dE galaxies and do not reveal an 'upturn' in their dynamical-to-stellar mass ratio as seen for the apparently dark matter dominated dSph galaxies.

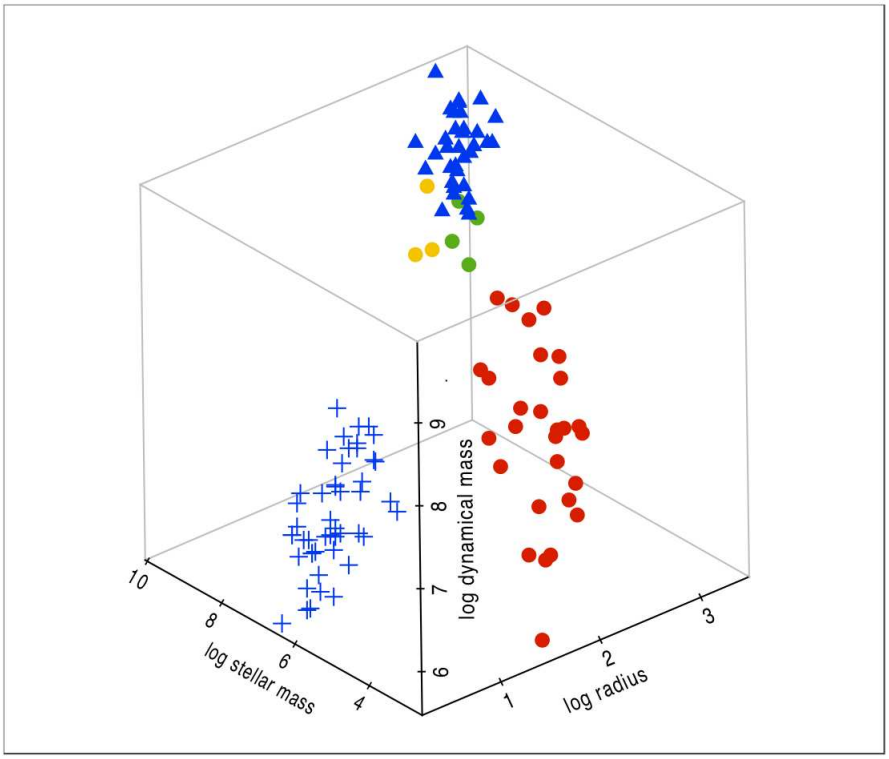

Figure 12. 3D manifold for dwarf systems. The axes are effective radius, dynamical mass and stellar mass. Our new data are shown by green dots, Local Group dEs by yellow dots, Virgo dEs by blue trainagles, UCDs by blue crosses and Local Group dSph galaxies by red circles. Our new data for low mass dE galaxies reveals a continuous trend from higher mass dEs to dSph galaxies.